

## Anisotropic flow of (multi-)strange hadrons in Au+Au collisions in BES-II energies at STAR.

---

**Prabhupada Dixit (for the STAR collaboration)<sup>a,\*</sup>**

<sup>a</sup>*Indian Institute of Science Education and Research (IISER) Berhampur,  
Berhampur, India*

*E-mail:* [prabhupadad@iiserbpr.ac.in](mailto:prabhupadad@iiserbpr.ac.in)

In this paper, we report the elliptic ( $v_2$ ) and triangular ( $v_3$ ) flow measurements of strange and multi-strange hadrons such as  $K_S^0$ ,  $\Lambda(\bar{\Lambda})$ ,  $\phi$ ,  $\Xi^-(\bar{\Xi}^+)$ , and  $\Omega^-(\bar{\Omega}^+)$  at mid-rapidity ( $|y| < 1.0$ ) in Au+Au collisions at  $\sqrt{s_{NN}} = 19.6$  GeV using high statistics Beam Energy Scan Phase-II (BES-II) data. The transverse momentum ( $p_T$ ) dependence, centrality dependence, and the number of constituent quarks (NCQ) scaling of  $v_2$  and  $v_3$  are studied for all these particles. A better NCQ scaling is observed in the case of antiparticles compared to particles, which can be attributed to the contribution from the transported quarks in particles. The hydrodynamically motivated ratio ( $v_3/v_2^{3/2}$ ) is presented as a function of  $p_T$ .

*41st International Conference on High Energy physics - ICHEP2022  
6-13 July, 2022  
Bologna, Italy*

---

\*Speaker

## 1. Introduction

Relativistic heavy-ion collisions provide the opportunity to study matter under extreme conditions of temperature and density where the quarks and gluons are no longer bound inside the hadrons. The azimuthal anisotropic flow of the final-state particles is an important observable for studying the initial stages and hydrodynamic evolution of the medium formed in such collisions. The anisotropic flow can be measured using Fourier series expansion of the azimuthal distributions of the particle yield in the momentum space given by

$$E \frac{d^3N}{dp^3} = \frac{1}{2\pi} \frac{d^2N}{p_T dp_T dy} \left[ 1 + \sum_n 2v_n \cos n(\phi - \psi_n) \right]. \quad (1)$$

Here,  $v_n$  represents the  $n^{\text{th}}$  order flow coefficient and  $\psi_n$  is the  $n^{\text{th}}$  order event plane angle. The second order coefficient ( $v_2$ ) and third order coefficient ( $v_3$ ) are known as elliptic and triangular flow, respectively. The  $n^{\text{th}}$  order flow coefficient can be measured by

$$v_n = \frac{\langle \cos n(\phi - \psi_n^{\text{obs}}) \rangle}{\langle \cos n(\psi_n^{\text{obs}} - \psi_n) \rangle}. \quad (2)$$

Here, the denominator represents the event plane resolution, the factor that takes the deviation of the observed  $n^{\text{th}}$  order event plane angle and the true  $n^{\text{th}}$  harmonic plane angle ( $\psi_n$ ). The angular bracket represents the average over all the particles in the event and over all the events. Various model studies [1–3] proposed that  $v_2$  and  $v_3$  are sensitive to the equation of the state and quantities characterizing the transport properties of the medium, such as the shear viscosity to entropy density ratio ( $\eta/s$ ).

Multi-strange hadrons and  $\phi$  mesons have small hadronic interaction cross sections and they freeze out early from the medium [4]. They are least affected by the late hadronic stage of the medium and are considered as excellent probes for the initial stages of the system. Prior to the RHIC BES-II program, the STAR detectors were upgraded to have an extended pseudorapidity coverage and better particle identification capabilities. The pseudorapidity coverage becomes wider ( $|\eta| < 1.5$ ) compared to BES-I ( $|\eta| < 1.0$ ) by upgrading the inner TPC (iTTPC). The statistics of the event sample are improved by a factor of 30 for Au+Au collisions at  $\sqrt{s_{NN}} = 19.6$  GeV compared to BES-I, which enables us to obtain more precise measurements of  $v_2$  and  $v_3$  of multi-strange hadrons and  $\phi$  mesons at low energy regimes.

## 2. Analysis details

First, we need to measure the event plane angle  $\psi_n$  which is given by

$$\psi_n = \frac{1}{n} \tan^{-1} \frac{\sum_i w_i \sin(n\phi_i)}{\sum_i w_i \cos(n\phi_i)}. \quad (3)$$

Here,  $\phi_i$  is the azimuthal angle of the  $i^{\text{th}}$  particle. The weight factor  $w_i = p_T \times \phi$ -weight is applied to optimize the event plane resolution and to take care of the non-uniform acceptance in  $\phi$ . Here, the factor for  $\phi$ -weight is obtained from the inverse of the azimuthal distribution ( $dN/d\phi$ ) of the

particles which is used to make the event plane angle distribution isotropic. The details of  $\phi$ -weight estimation can be found in Ref. [5]. Experimentally, the event plane resolution is given by

$$R_n = \sqrt{\langle \cos n(\psi_n^A - \psi_n^B) \rangle}. \quad (4)$$

Here  $\psi_n^A$  and  $\psi_n^B$  are two sub-event planes in the opposite pseudorapidity ( $\eta$ ) sides of  $\eta$  coverage  $-1.5 < \eta < -0.05$  and  $0.05 < \eta < 1.5$  respectively and  $R_n$  is the sub-event plane resolution. Figure 1 shows  $R_n$  as a function of centrality. The resolution of  $\psi_2$  is about 10% higher compared to that of the BES-I measurement [6]. We use the invariant mass method [7] to measure the  $v_n$  of the short-lived

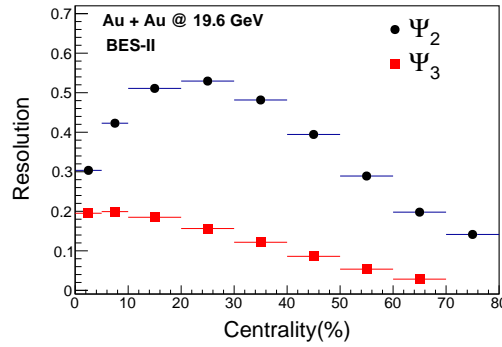


**Figure 1:** Sub-event plane resolutions for  $\psi_2$  and  $\psi_3$  are shown as a function of centrality. Both TPC and iTPC are used to construct the event planes.

particles used in this analysis. A detailed procedure for the method can be found in Refs. [8, 9].

### 3. Results

#### 3.1 $p_T$ dependence of $v_2$

Figure 2 shows  $v_2$  of particles and anti-particles as a function of  $p_T$  in 10-40% centrality for all the (multi-)strange hadrons such as  $K^+(K^-)$ ,  $K_S^0$ ,  $\Lambda(\bar{\Lambda})$ ,  $\Xi^-(\bar{\Xi}^+)$ ,  $\Omega^-(\bar{\Omega}^+)$ , and  $\phi$  mesons along with non-strange hadrons such as  $\pi^+(\pi^-)$  and  $p(\bar{p})$ . We observe a mass ordering in the lower  $p_T$  ( $p_T < 1.5$  GeV/ $c$ ) region, that is, lighter mass particles show higher  $v_2$  due to the radial flow of the system [10]. Above  $p_T > 1.5$  GeV/ $c$ , baryon-meson separation is observed, consistent with the picture of the coalescence model of hadronization [11]. The statistical error bars in the BES-II measurements are about three times smaller than those in the BES-I measurements.

#### 3.2 Centrality dependence of $v_2$ and $v_3$

The centrality dependence of  $v_2$  and  $v_3$  are studied. As shown in Fig. 3,  $v_2$  shows a strong centrality dependence for all particles. This indicates that  $v_2$  arises predominantly from spatial anisotropy in the overlap region of the colliding nuclei. The centrality dependence of  $v_3$  is weak, as shown in Fig. 4. This is due to the fact that the dominant cause of  $v_3$  is the event-by-event fluctuation of the energy density in the overlap region of the two nuclei.

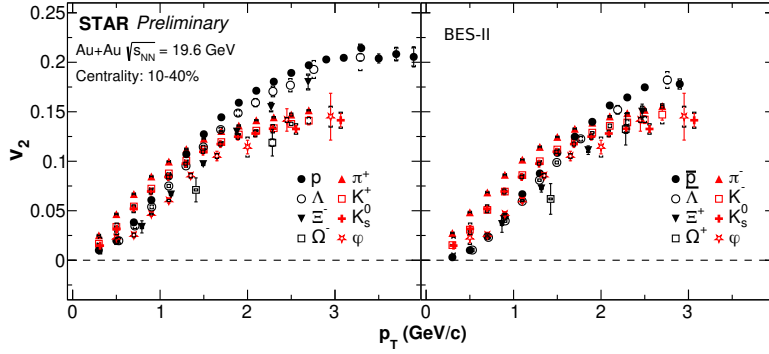


**Figure 2:** The left panel shows  $v_2$  of particles as a function of  $p_T$  for the 10-40% centrality. The right panel shows the same for antiparticles. The vertical lines and caps represent the statistical uncertainties and systematic uncertainties, respectively.

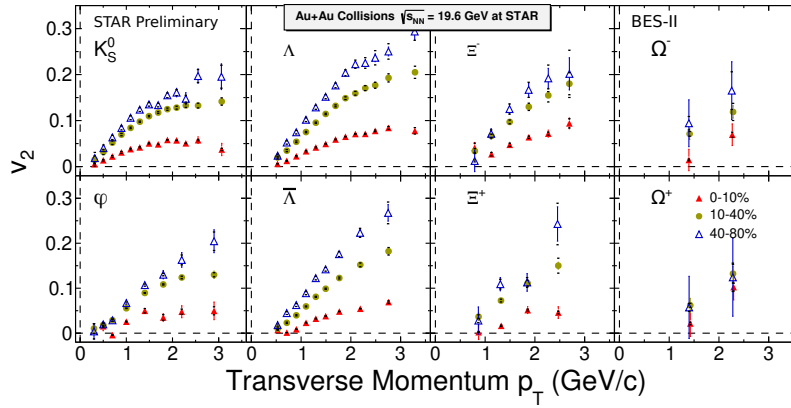


**Figure 3:**  $v_2$  as a function of  $p_T$  for three different centrality classes, 0-10%, 10-40%, and 40-80%. The vertical lines and caps represent the statistical uncertainties and systematic uncertainties, respectively.

### 3.3 Number of constituent quarks scaling in $v_3$

Figure 5 shows the modified NCQ-scaled  $v_3$ , i.e.,  $v_3/n_q^{3/2}$  [12], as a function of NCQ-scaled transverse kinetic energy  $(m_T - m_0)/n_q$  for all particles (left) and antiparticles (right), respectively. The  $K_S^0$  data points are fitted with a third-order polynomial and the ratios of  $v_3/n_q^{3/2}$  of all other particles (antiparticles) are taken with respect to the fit function of  $K_S^0$ . To quantify the scaling, the ratios are fitted simultaneously with a polynomial of order zero. It is observed that the scaling holds within 15% for antiparticles and within 30% for particles. The scaling is better for antiparticles than for particles; this could be due to the effect from transported quarks in particles. The picture is consistent with NCQ-scaled  $v_2$  measured from BES-II data at 19.6 GeV [13].

### 3.4 $v_3/v_2^{3/2}$ ratio

The hydrodynamics-motivated ratio of  $v_3/v_2^{3/2}$  is suggested to be independent of  $p_T$  and its magnitude is sensitive to the transport properties of the medium [14–16]. Figure 6 shows the ratio

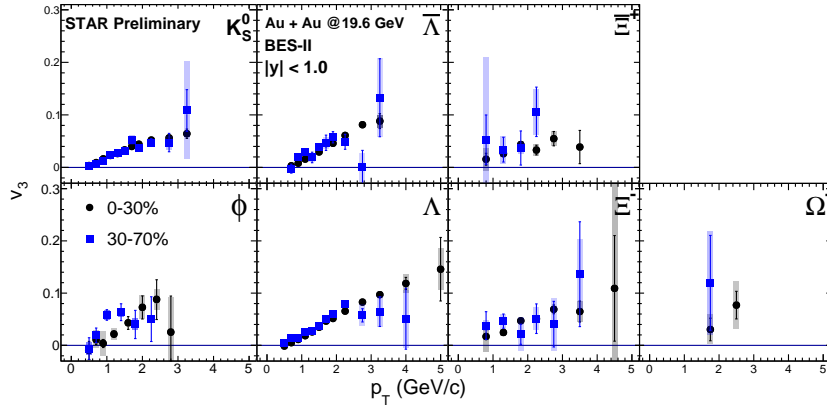


**Figure 4:**  $v_3$  as a function of  $p_T$  for two different centrality classes, 0-30% and 30-70%. The vertical lines and shaded boxes represent the statistical uncertainties and systematic uncertainties, respectively.

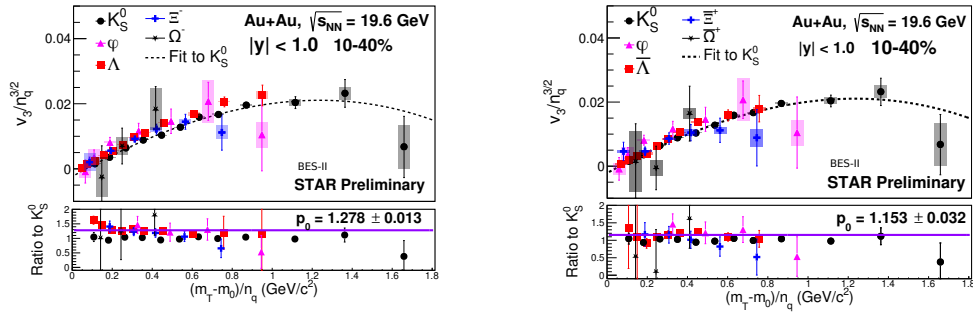


**Figure 5:** Left figure shows the  $v_3/n_q^{3/2}$  as a function of the NCQ scaled  $m_T - m_0$  for particles in 10-40% centrality class. The lower left panel shows the straight line fit to the scaled  $v_3$  ratios taken with respect to the  $K_S^0$  fit line. Right figure shows the same for the antiparticles. The vertical lines and shaded boxes represent the statistical uncertainties and systematic uncertainties, respectively.

$v_3/v_2^{3/2}$  as a function of  $p_T$  in 10-40% centrality. The ratio shows a weak dependence on  $p_T$  above 1.5 GeV/c for all the particle species.

#### 4. Summary

In summary, we report the elliptic flow and triangular flow of (multi-)strange hadrons and  $\phi$  meson in Au+Au collisions at  $\sqrt{s_{NN}} = 19.6$  GeV using the high-statistics BES-II data. The  $p_T$  dependence of  $v_2$  shows a mass ordering at  $p_T < 1.5$  GeV/c and a particle-type separation at  $p_T > 1.5$  GeV/c, which depends on the valence quark content of the particle species. The centrality dependence of  $v_2$  and  $v_3$  is studied. The  $v_2$  shows strong centrality dependence for all the particle species to be driven by the centrality dependence of initial ellipticity. Unlike  $v_2$ , the centrality dependence in  $v_3$  is weak because it is expected to be driven by initial state fluctuations. The modified NCQ scaling for  $v_3$  is found to hold better for antiparticles compared to particles, which can be attributed to the effect of transported quarks initially present in the colliding system. A weak

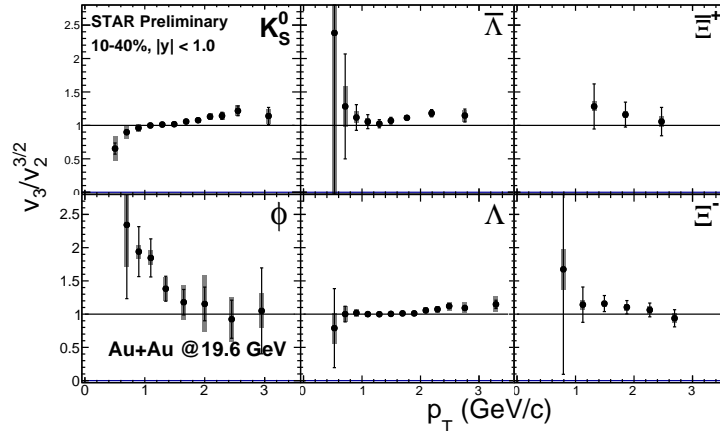


**Figure 6:**  $v_3/v_2^{3/2}$  as a function of  $p_T$  in the 10-40% centrality for  $K_S^0$ ,  $\Lambda(\bar{\Lambda})$ ,  $\phi$ , and  $\Xi^-(\bar{\Xi}^+)$ . The vertical lines and shaded boxes represent the statistical uncertainties and systematic uncertainties, respectively.

$p_T$  dependence of hydrodynamics-motivated ratio,  $v_3/v_2^{3/2}$ , is observed for all the particles above  $p_T > 1.5$  GeV/c.

## References

- [1] J. Y. Ollitrault, Phys. Rev. D **46**, 229 (1992)
- [2] C. Shen and U. Heinz, Phys. Rev. C **85**, 054902 (2012)
- [3] C. Shen *et al.*, J. Phys. G: Nucl. Part. Phys. **38**, 124045 (2011)
- [4] A. Shor, Phys. Rev. Lett. **54**, 1122 (1985)
- [5] A. M. Poskanzer and S. A. Voloshin, Phys. Rev. C **58**, 1671 (1998)
- [6] L. Adamczyk *et al.* (STAR), Phys. Rev. C **88**, 14902 (2013)
- [7] N. Borghini and J.-Y. Ollitrault, Phys. Rev. C **70**, 064905 (2004)
- [8] STAR, arXiv:2205.11073 [hep-ex]
- [9] P. Dixit (STAR), arXiv:2103.04646 [hep-ex]
- [10] D. Teaney, J. Lauret, and E. V. Shuryak, Phys. Rev. Lett. **86**, 4783 (2001)
- [11] D. Molnar and S. A. Voloshin, Phys. Rev. Lett. **91**, 092301 (2003)
- [12] L. X. Han *et al.*, Phys. Rev. C **84**, 064907 (2011)
- [13] L. Liu (STAR), arXiv:2208.14604 [hep-ex]
- [14] E. Retinskaya, M. Luzum, and J.-Y. Ollitrault, Phys.Rev. C **89**, 014902 (2014)
- [15] E. Retinskaya, M. Luzum, and J.-Y. Ollitrault, Nucl. Phys. A **926**, 152 (2014)
- [16] C. Lang and N. Borghini, Eur.Phys.J. C **74**, 2955 (2014)